Molecular Cell, Volume *72*

Supplemental Information

The Chromatin Reader ZMYND8 Regulates *Igh* Enhancers to Promote Immunoglobulin Class Switch Recombination

Verónica Delgado-Benito, Daniel B. Rosen, Qiao Wang, Anna Gazumyan, Joy A. Pai, Thiago Y. Oliveira, Devakumar Sundaravinayagam, Wenzhu Zhang, Matteo Andreani, Lisa Keller, Kyong-Rim Kieffer-Kwon, Aleksandra Pękowska, Seolkyoung Jung, Madlen Driesner, Roman I. Subbotin, Rafael Casellas, Brian T. Chait, Michel C. Nussenzweig, and Michela Di Virgilio

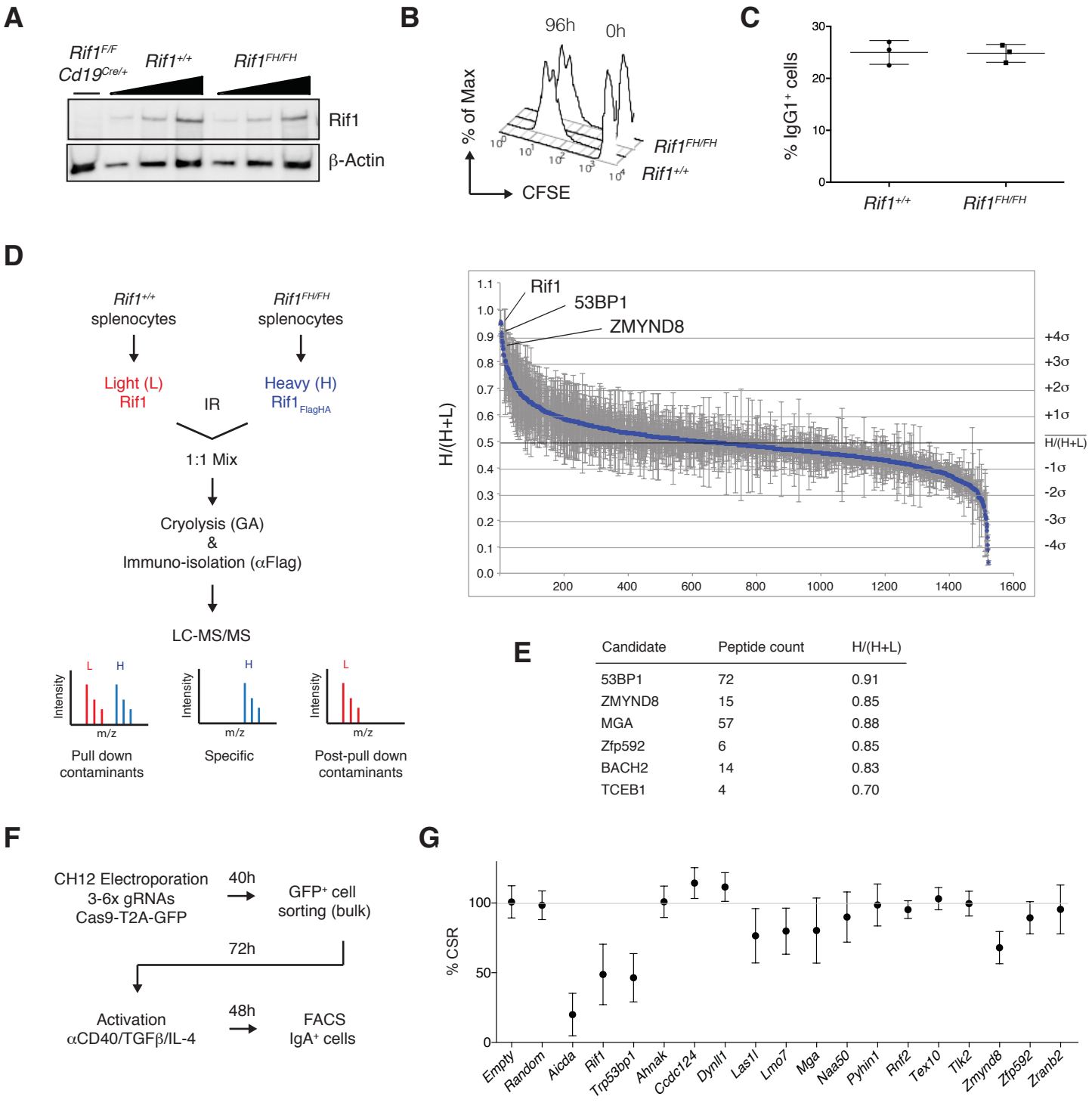

Candidate	Peptide count	H/(H+L)
53BP1	72	0.91
ZMYND8	15	0.85
MGA	57	0.88
Zfp592	6	0.85
BACH2	14	0.83
TCEB1	4	0.70

Figure S1

Figure S1. Identification of Rif1 interacting proteins in primary B cells undergoing CSR, Related to Figure 1. (A) Western blot analysis of whole cell extracts from *WT (Rif1*$^{+/+}$*)* and *Rif1*$^{FH/FH}$ splenocytes. Triangles indicate threefold dilution. (B) Flow cytometry histograms measuring B cell proliferation by CFSE-dye dilution 96 h after stimulation with LPS, IL-4 and RP/14. (C) Summary dot plot for three independent experiments (n = three mice per genotype) measuring CSR to IgG1 96 hours after stimulation of B lymphocytes with LPS, IL-4 and RP/14. (D) Left: scheme of Rif1 I-DIRT in primary cultures of splenocytes. IR: ionizing radiation; GA: glutaraldehyde; LC-MS/MS: liquid chromatography-tandem mass spectrometry. Right: Graph depicting the distribution of identified Rif1 I-DIRT proteins as a function of their H/(H+L) ratio. Error bars represent the standard error of each candidate H/(H + L) mean value. Only proteins with peptide count ≥ 4 and posterior error probability (PEP) ≤ 10^{-4} were included).

$\overline{H/(H+L)}$ and σ are the mean (0.49) and standard deviation (0.10) of the distribution, respectively. (E) Potential Rif1 interactors identified among top I-DIRT hits. (F) Schematic representation of the screen for loss-of-CSR following somatic targeting *via* CRISPR-Cas9 in CH12 cells. (G) Graph depicting residual CSR levels (% IgA^{+} cells) measured after somatic targeting of the indicated I-DIRT hits in bulk CH12 cultures. The graph summarizes at least three independent experiments for each candidate. (H-I) Western blot analysis of anti-Flag(Rif1) (H), and anti- ZMYND8 (I) immunoprecipitates from *WT* and *Rif1*$^{FH/FH}$ B lymphocytes either left untreated or irradiated (10 gray (Gy), 45-min recovery) in the presence or absence of the ATM kinase inhibitor KU55933 (ATMi). Data are representative of at least two independent experiments for each co-immunoprecipitation.

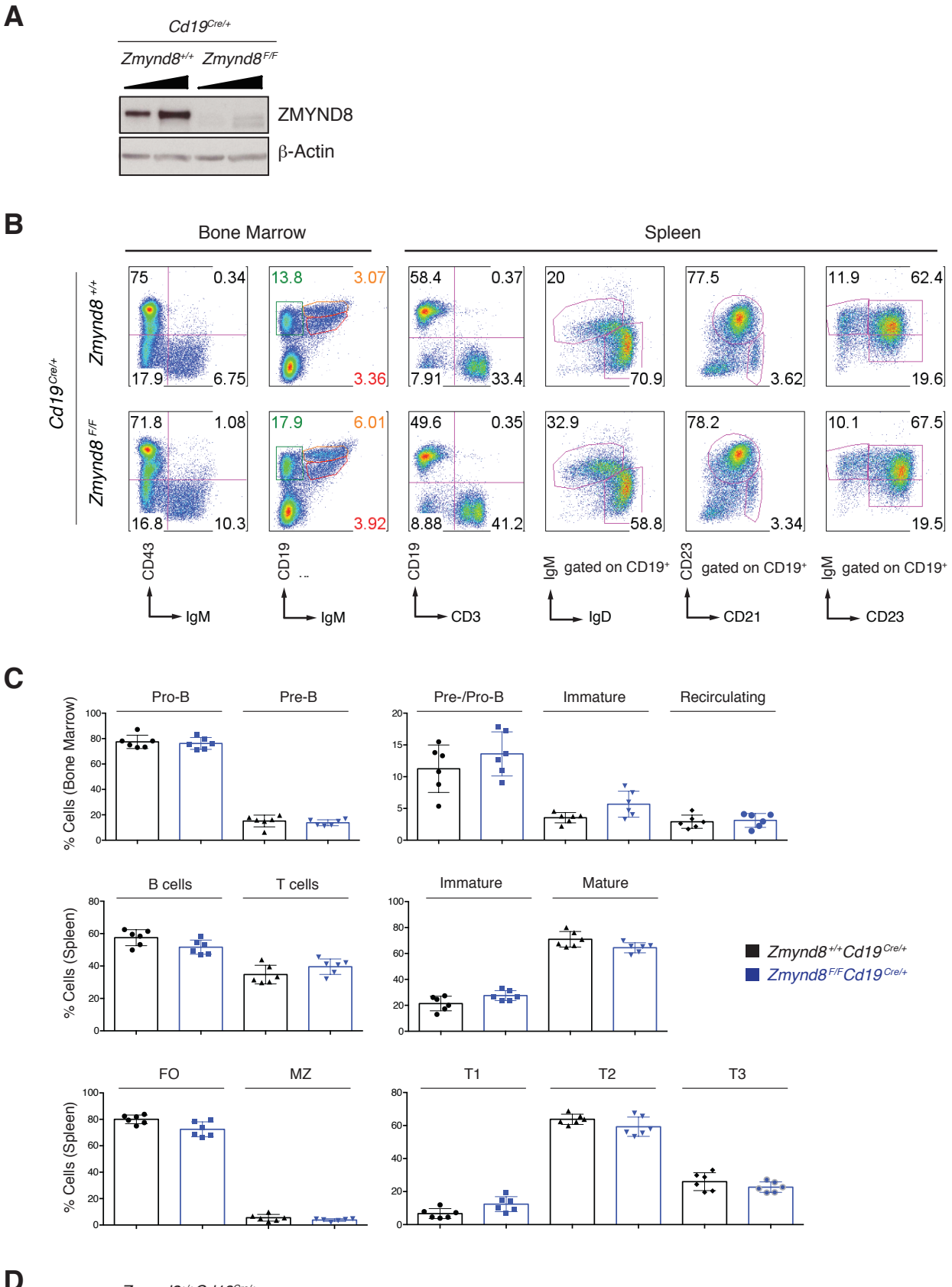
A
Cd19Cre/+
Zmynd8+/+ Zmynd8F/F
ZMYND8
β-Actin
B
Bone Marrow
Spleen
Cd19Cre/+
Zmynd8 +/+
Zmynd8 F/F
75 0.34 17.9 6.75
13.8 3.07 3.36
58.4 0.37 7.91 33.4
20 70.9
77.5 3.62
11.9 62.4 19.6
71.8 1.08 16.8 10.3
17.9 6.01 3.92
49.6 0.35 8.88 41.2
32.9 58.8
78.2 3.34
10.1 67.5 19.5
CD43 IgM
CD19 IgM
CD19 CD3
IgM gated on CD19+ IgD
CD23 gated on CD19+ CD21
IgM gated on CD19+ CD23
C
Pro-B
Pre-B
Pre-/Pro-B
Immature
Recirculating
% Cells (Bone Marrow)
B cells
T cells
Immature
Mature
% Cells (Spleen)
Zmynd8+/+Cd19Cre/+
Zmynd8F/FCd19Cre/+
FO
MZ
T1
T2
T3
% Cells (Spleen)
D
Zmynd8+/+Cd19Cre/+
0 48 72 h
ZMYND8
β-Actin

Figure S2

Figure S2. ZMYND8 is dispensable for B cell development, Related to Figure 2. (A) Western blot analysis of whole cell extracts from *Cd19*$^{Cre/+}$ and *Zmynd8*$^{F/F}$*Cd19*$^{Cre/+}$ B cells 72 h after stimulation with LPS and IL-4. Triangles indicate threefold dilution. (B) Representative flow cytometry analysis of lymphoid tissues from *Cd19*$^{Cre/+}$ and *Zmynd8*$^{F/F}$*Cd19*$^{Cre/+}$ mice. (C) Summary graphs for six mice per genotype. (D) Western blot analysis of whole cell extracts from mature *Cd19*$^{Cre/+}$ B cells in resting conditions (0 h) and at the indicated times after stimulation with LPS and IL-4.

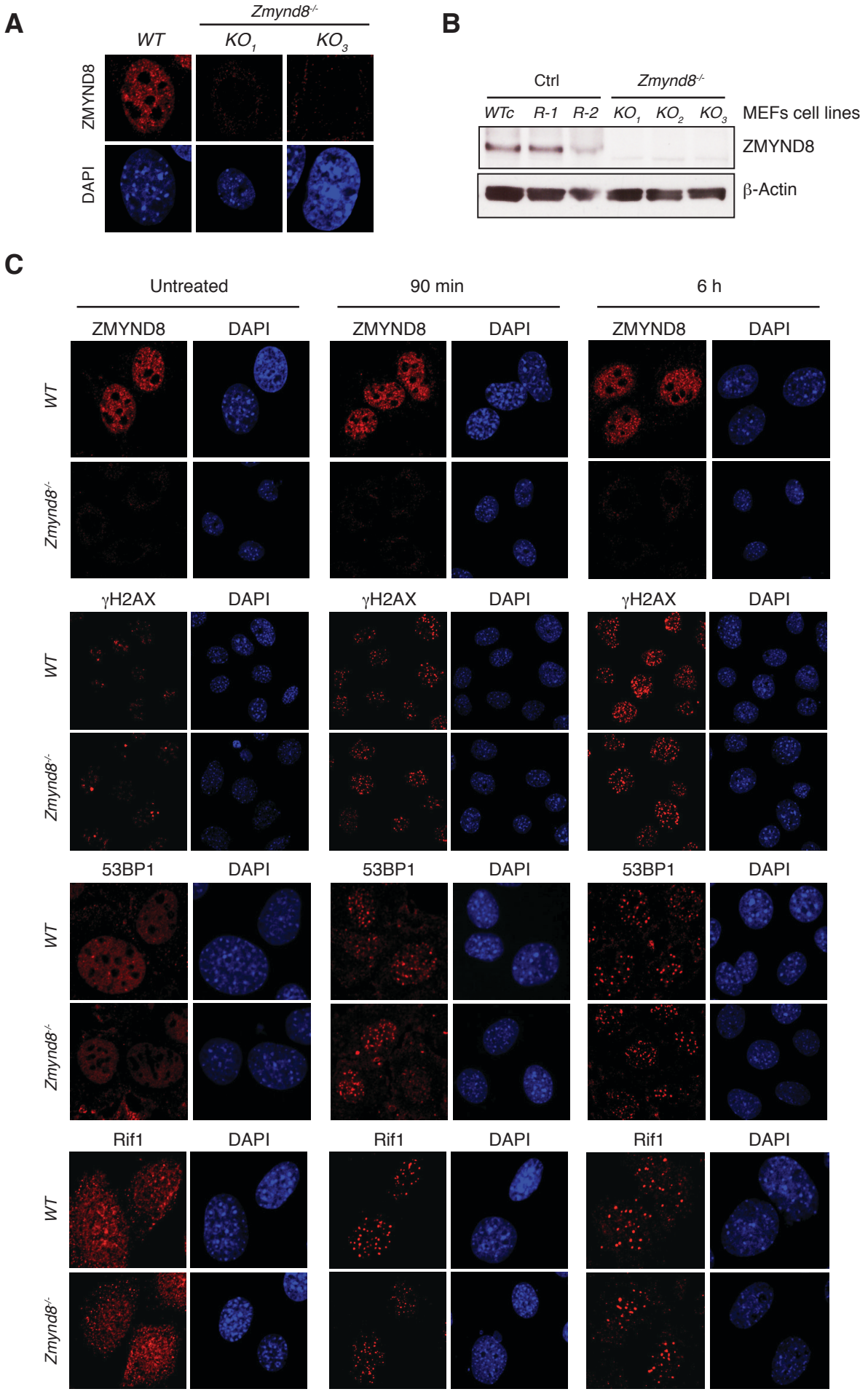
A
Zmynd8-/-
WT
KO1
KO3
ZMYND8
DAPI
B
Ctrl
Zmynd8-/-
WTc
R-1
R-2
KO1
KO2
KO3
MEFs cell lines
ZMYND8
β-Actin
C
Untreated
90 min
6 h
ZMYND8
DAPI
γH2AX
53BP1
Rif1
WT
Zmynd8-/-

Figure S3

Figure S3. ZMYND8-deficiency does not affect DSB-induced signaling, Related to Figures 1, 2, and S1. (A-B) Immunofluorescent staining (A) and WB (B) analysis of *Zmynd8*$^{-/-}$ immortalized mouse embryonic fibroblast (iMEF) clonal cell lines. Ctrl iMEFs cell lines include a WT clonal derivative (WTc) and two clones generated by targeting iMEFs cells with a random sequence not present in the mouse genome (R-1 and R-2). *KO*$_1$, *KO*$_2$, and *KO*$_3$ are three independent *Zmynd8*$^{-/-}$ iMEFs cell lines. (C) Immunofluorescent staining for ZMYND8, γH2AX, 53BP1, and Rif1 in irradiated (10 Gy) *Zmynd8*$^{-/-}$ (*KO*$_1$ clone) iMEFs. Data are representative of two independent experiments.

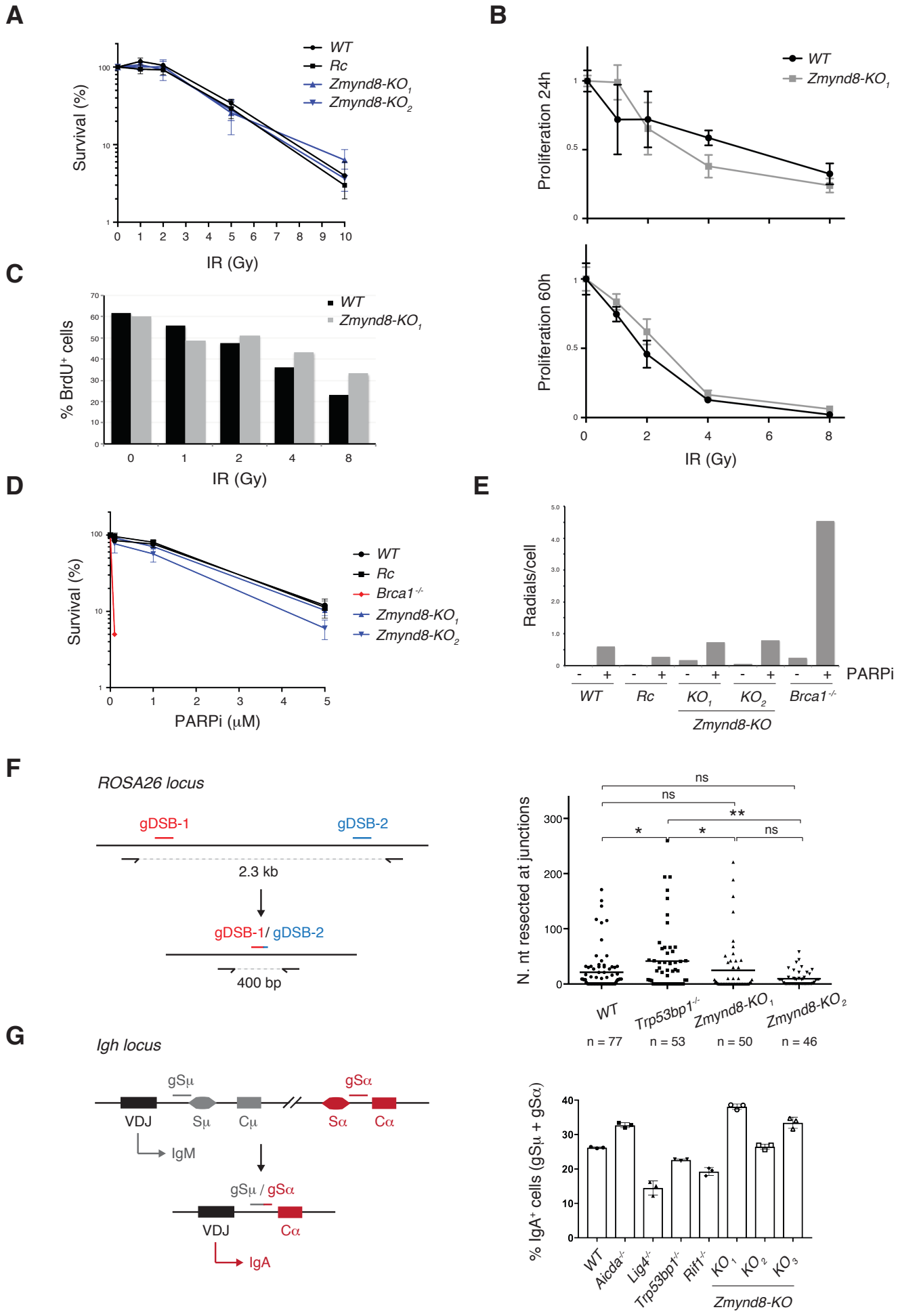
A
Survival (%)
IR (Gy)
WT
Rc
Zmynd8-KO1
Zmynd8-KO2
B
Proliferation 24h
Proliferation 60h
IR (Gy)
WT
Zmynd8-KO1
C
% BrdU+ cells
IR (Gy)
WT
Zmynd8-KO1
D
Survival (%)
PARPi (μM)
WT
Rc
Brca1-/-
Zmynd8-KO1
Zmynd8-KO2
E
Radials/cell
PARPi
WT
Rc
KO1
KO2
Brca1-/-
Zmynd8-KO
F
ROSA26 locus
gDSB-1
gDSB-2
2.3 kb
gDSB-1/ gDSB-2
400 bp
N. nt resected at junctions
ns
*
**
WT
Trp53bp1-/-
Zmynd8-KO1
Zmynd8-KO2
n = 77
n = 53
n = 50
n = 46
G
Igh locus
gSμ
gSα
VDJ
Sμ
Cμ
Sα
Cα
IgM
gSμ / gSα
IgA
% IgA+ cells (gSμ + gSα)
WT
Aicda-/-
Lig4-/-
Trp53bp1-/-
Rif1-/-
KO1
KO2
KO3
Zmynd8-KO

Figure S4

Figure S4. *Zmynd8*$^{-/-}$ CH12 and MEFs cell lines do not exhibit major DSB repair defects, Related to Figures 1, 2, and S1. (A) Colony formation assay of two independent *Zmynd8*$^{-/-}$ iMEF clones (*KO*$_1$ and *KO*$_2$) following IR. Error bars represent the mean from triplicate plates per condition. Data are representative of two independent experiments. (B) Growth curves of WT and *Zmynd8*$^{-/-}$ CH12 cells after irradiation. (C) Cell cycle analysis of irradiated *Zmynd8*$^{-/-}$ CH12 lines as measured by BrdU incorporation. (D) Colony formation assay of *Zmynd8*$^{-/-}$ iMEF clones following PARPi treatment. Error bars represent the mean from triplicate plates per condition. Data are representative of two independent experiments. (E) Analysis of genomic instability in metaphases from PARPi (2 μM) -treated *Zmynd8*$^{-/-}$ iMEFs (n >= 42 metaphases analyzed per genotype). (F) Left: Schematic representation of the end resection assay. Right: Dot plot showing resection in sequences from joining products of two CRISPR-Cas9-induced DSBs at the *ROSA26* locus in two *Zmynd8*$^{-/-}$ CH12 cell lines (*KO*$_1$ and *KO*$_2$). Each dot represents one junction product. Number of junctions analyzed per genotype is indicated below. p values were calculated with the Mann–Whitney U test. n.s.: not significant. nt: nucleotide. (G) Left: Schematic representation of CRISPR-Cas9-induced CSR assay. Right: Summary dot plot for three independent experiments measuring CSR to IgA after electroporation of unactivated CH12 cells lines of the indicated genotypes with WT Cas9 and gRNAs against Random or Sα and Sμ sequences. *KO*$_1$, *KO*$_2$, and *KO*$_3$ are three independent *Zmynd8*$^{-/-}$ CH12 cell lines.

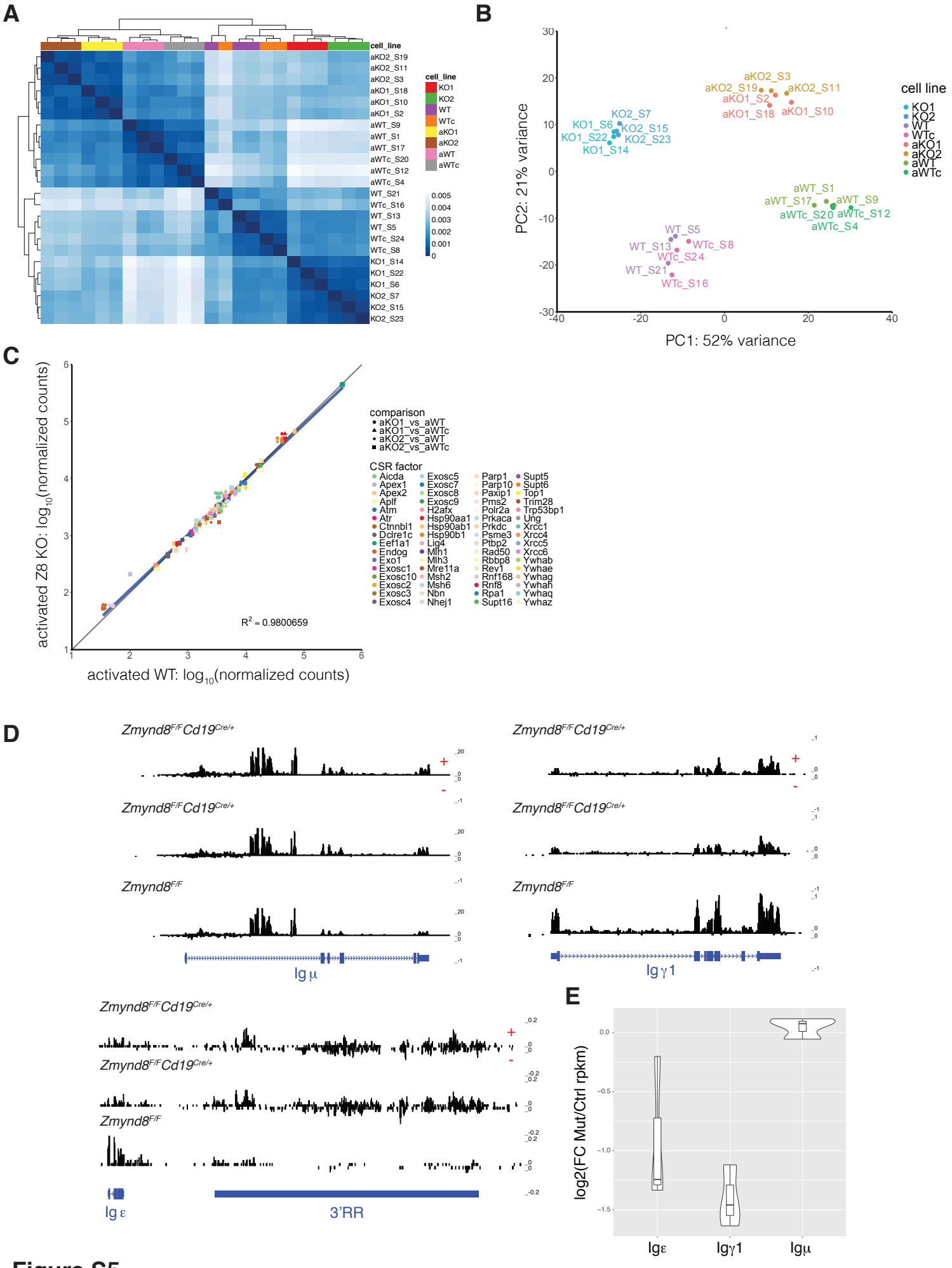
A
cell_line
aKO2_S19
aKO2_S11
aKO2_S3
aKO1_S18
aKO1_S10
aKO1_S2
aWT_S9
aWT_S1
aWT_S17
aWTc_S20
aWTc_S12
aWTc_S4
WT_S21
WTc_S16
WT_S13
WT_S5
WTc_S24
WTc_S8
KO1_S14
KO1_S22
KO1_S6
KO2_S7
KO2_S15
KO2_S23
cell_line
KO1
KO2
WT
WTc
aKO1
aKO2
aWT
aWTc
0.005
0.004
0.003
0.002
0.001
0
B
PC2: 21% variance
PC1: 52% variance
cell line
KO1
KO2
WT
WTc
aKO1
aKO2
aWT
aWTc
C
activated Z8 KO: log10(normalized counts)
activated WT: log10(normalized counts)
R2 = 0.9800659
comparison
aKO1_vs_aWT
aKO1_vs_aWTc
aKO2_vs_aWT
aKO2_vs_aWTc
CSR factor
Aicda
Apex1
Apex2
Aplf
Atm
Atr
Ctnnbl1
Dclre1c
Eef1a1
Endog
Exo1
Exosc1
Exosc10
Exosc2
Exosc3
Exosc4
Exosc5
Exosc7
Exosc8
Exosc9
H2afx
Hsp90aa1
Hsp90ab1
Hsp90b1
Lig4
Mlh1
Mlh3
Mre11a
Msh2
Msh6
Nbn
Nhej1
Parp1
Parp10
Paxip1
Pms2
Polr2a
Prkaca
Prkdc
Psme3
Ptbp2
Rad50
Rbbp8
Rev1
Rnf168
Rnf8
Rpa1
Supt16
Supt5
Supt6
Top1
Trim28
Trp53bp1
Ung
Xrcc1
Xrcc4
Xrcc5
Xrcc6
Ywhab
Ywhae
Ywhag
Ywhah
Ywhaq
Ywhaz
D
Zmynd8F/FCd19Cre/+
Zmynd8F/F
Ig μ
Ig γ1
Ig ε
3'RR
E
log2(FC Mut/Ctrl rpkm)
Igε
Igγ1
Igμ

Figure S5

Figure S5. ZMYND8-deficiency impairs GLT of acceptor S regions but does not reduce the expression of known CSR factors, Related to Figures 1, 3, and 5. (A-B) Dendrogram (A) and Principal Component Analysis (B) for WT CH12 cells (bulk and one clonal derivative WTc) and two *Zmynd8*$^{-/-}$ cell lines (*KO1* and *KO2*) under either unactivated or activated conditions (prefix "a" indicates stimulation for 48 h with αCD40, TGFβ and IL-4). RNA-Seq analysis was performed on three biological replicates per condition. (C) Scatterplot for gene expression of known CSR factors in activated WT CH12 and *Zmynd8*$^{-/-}$ samples. Pairwise comparisons between WT and *Zmynd8*$^{-/-}$ cell lines are represented as different shapes, while CSR factors are denoted by color. Linear regression line shown in blue; identity line shown in grey. (D) GRO-Seq analysis of nascent RNA transcription at the indicated *Igh* regions in B lymphocytes stimulated for 24 h with LPS and IL-4. + and – indicate sense and antisense transcription, respectively. (E) Differential gene analysis of GRO-Seq data in panel D. pvalues were calculated with one-sided one sample t.test (mu=0) on log2FC (Igε: 0.0627, Igγ1: 0.0057, Igμ: 0.2319). Mean log2FC: Igε: -0.93, Igγ1: -1.41, Igμ: 0.047. Mut: mutant *Zmynd8*$^{F/F}$*Cd19*$^{Cre/+}$*;* Ctrl: control *Zmynd8*$^{F/F}$.

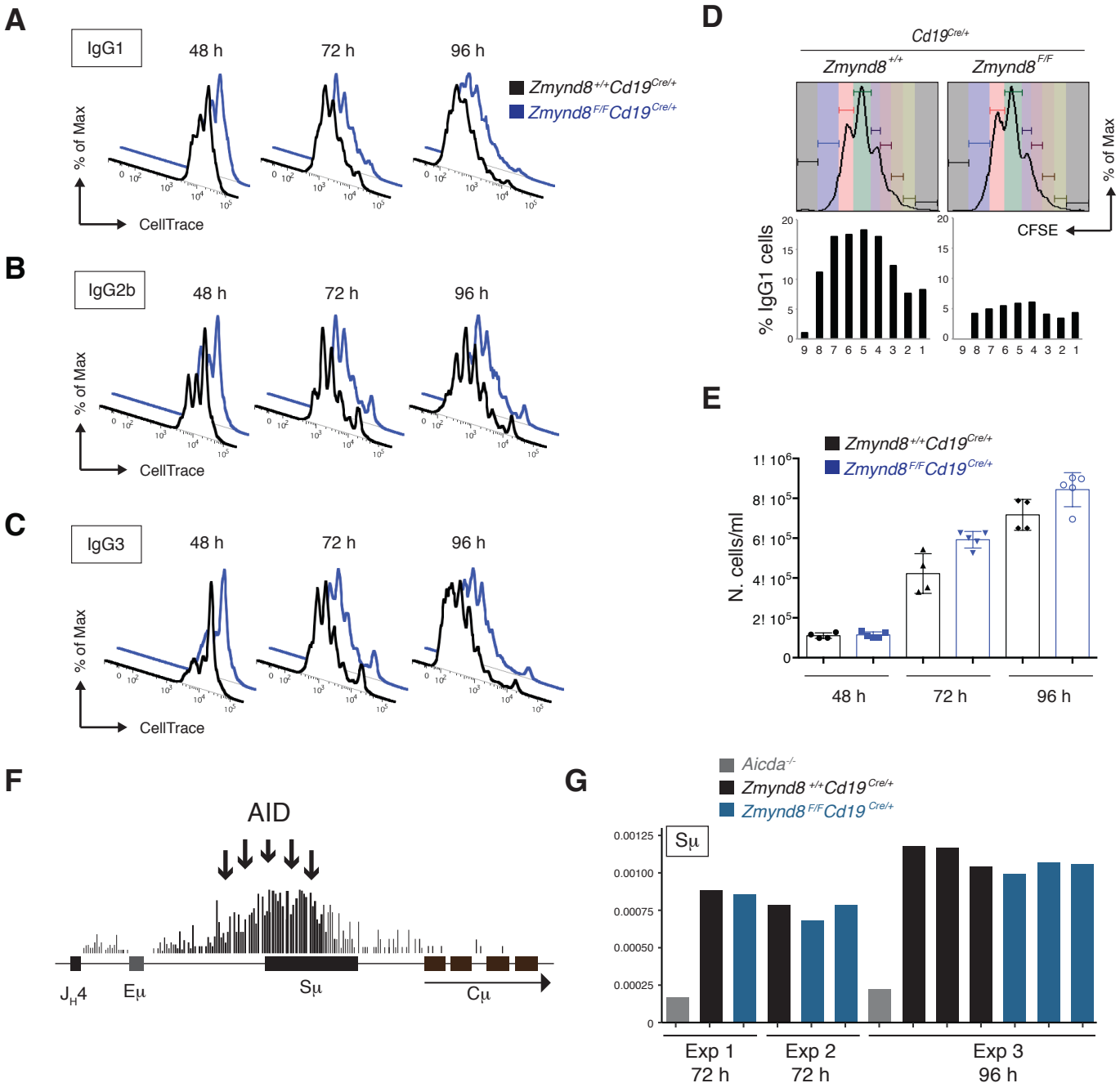
A
IgG1
48 h
72 h
96 h
Zmynd8+/+Cd19Cre/+
Zmynd8F/FCd19Cre/+
% of Max
CellTrace
B
IgG2b
C
IgG3
D
Cd19Cre/+
Zmynd8+/+
Zmynd8F/F
% of Max
CFSE
% IgG1 cells
E
N. cells/ml
F
AID
JH4
Eμ
Sμ
Cμ
G
Aicda-/-
Sμ
Exp 1
72 h
Exp 2
72 h
Exp 3
96 h

Figure S6

Figure S6. ZMYND8-deficiency does not affect B cell proliferation or the frequency of mutations at 5'Sμ, Related to Figures 2 and 6. (A-C) Proliferation analysis by CellTrace Violet dilution of primary cultures of *Cd19*$^{Cre/+}$ and *Zmynd8*$^{F/F}$*Cd19*$^{Cre/+}$ B lymphocytes stimulated with LPS and IL-4 (A), LPS-BAFF-TGFβ (B), or LPS only (C). Data are representative of at least two mice per genotype. (D) Representative flow cytometry analysis showing the percentage of IgG1^{+} cells per cell division in primary cultures of *Cd19*$^{Cre/+}$ and *Zmynd8*$^{F/F}$*Cd19*$^{Cre/+}$ splenocytes stimulated with LPS and IL-4 for 72 h. Cell division as measured by CFSE dye dilution is shown on top. (E) Growth curves of primary B cell cultures from *Cd19*$^{Cre/+}$ and *Zmynd8*$^{F/F}$*Cd19*$^{Cre/+}$ mice stimulated with LPS and IL-4. The graph summarizes two independent experiments with at least 4 mice per genotype tested in total. (F) Schematic representation of Eμ-Sμ-Cμ region with footprint of AID-induced mutations. (G) Histogram depicting cumulative mutation frequencies as determined by mutational analysis by paired-end deep-sequencing (MutPE-Seq) at 5'-Sμ in *CD19*$^{Cre/+}$, *Zmynd8*$^{F/F}$*CD19*$^{Cre/+}$, and *AID*$^{-/-}$ splenocytes 72 h or 96 h after activation with LPS and IL-4. Three independent experiments are shown with each bar representing a different mouse.

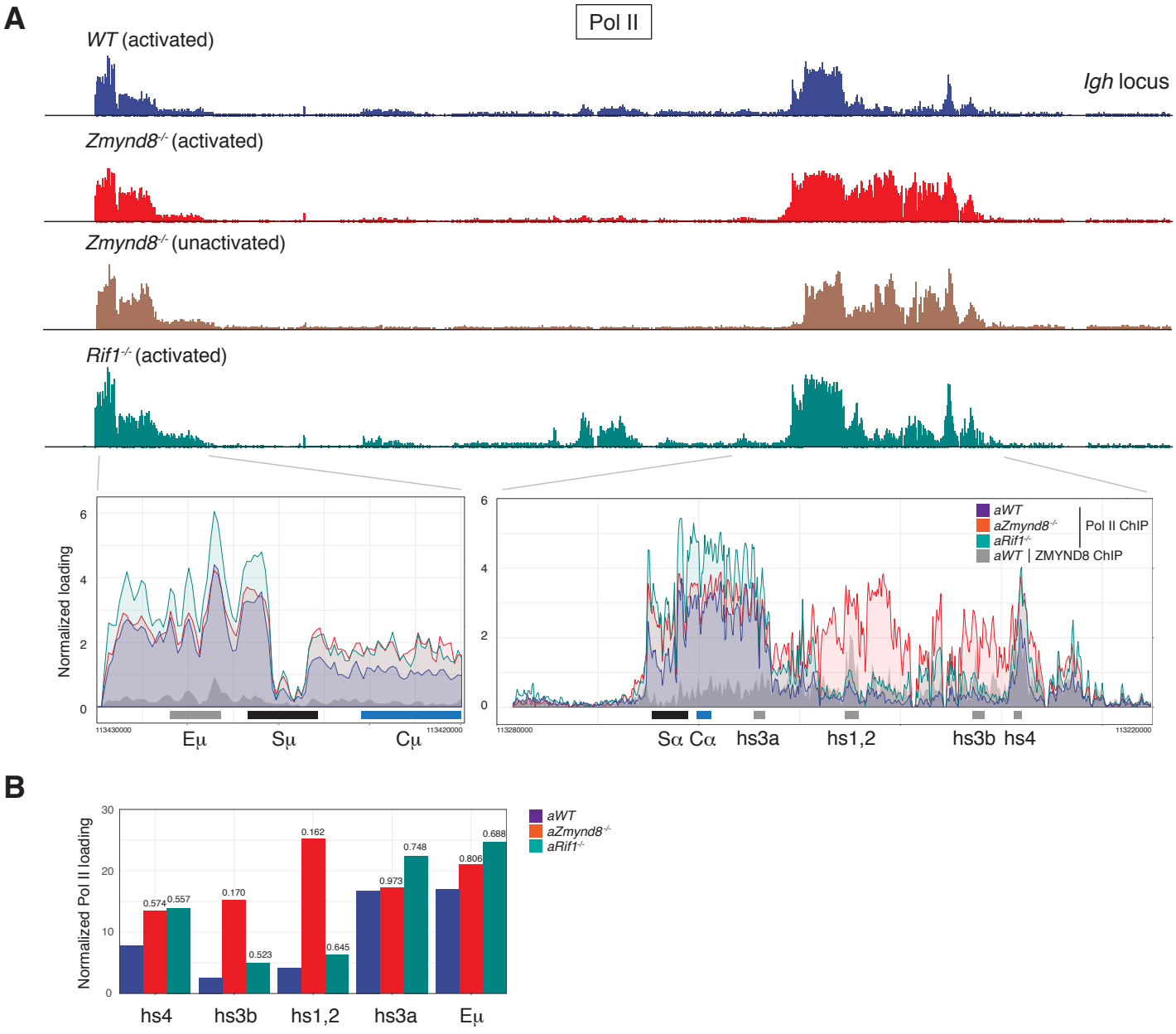
A
Pol II
WT (activated)
Igh locus
Zmynd8-/- (activated)
Zmynd8-/- (unactivated)
Rif1-/- (activated)
Normalized loading
Eμ
Sμ
Cμ
Sα Cα
hs3a
hs1,2
hs3b
hs4
aWT
aZmynd8-/-
aRif1-/-
Pol II ChIP
aWT | ZMYND8 ChIP

B
Normalized Pol II loading
aWT
aZmynd8-/-
aRif1-/-
0.574
0.557
0.170
0.523
0.162
0.645
0.973
0.748
0.806
0.688
hs4
hs3b
hs1,2
hs3a
Eμ

Figure S7

Figure S7. RNA Pol II loading is increased at the 3' *Igh* enhancers of ZMYND8-deficient CH12 cells, Related to Figures 4 and 5. (A) Top: RNA Pol II loading at the *Igh* locus in WT, *Zmynd8*$^{-/-}$, and *Rif1*$^{-/-}$ CH12 cells. Bottom: ChIP-Seq tracks overlay at regions encompassing Eμ and 3'RR enhancers. Regions zoomed-in in the insets were defined based on the location of ZMYND8 peaks from ZMYND8 ChIP-Seq in Fig. 4C (grey track). (B) RNA Pol II loading quantification at regions highlighted within the insets in panel A. Numbers above columns represent the ratio of RNA Pol II loading in WT to loading in knock-out cells. Prefix "a" indicates stimulation for 48 h with αCD40, TGFβ and IL-4.

Table S1. Sμ-Sγ1 junction recombination analysis in *Zmynd8$^{F/F}$Cd19$^{Cre/+}$* and control B cells, Related to Figure 2.

Sμ-Sγ1	*Cd19$^{Cre/+}$* (30N)	*Zmynd8$^{F/F}$Cd19$^{Cre/+}$* (29N)
Mouse #1	TTGAATAGAGCTAAACTCTACTGCCT**ACA**GGTGGGAGTGTGGGGATCCAGG CACAGCTGTACAGAATTGAGAAA***C***AAT**AG**GACAGGTGGGAGTGTGGGGATCCAGGT CGAGATGAGCCAAACTGGAATGAACTT:GTGTGGAGACCCAGGCAGAGCAGCTATA AAAGAATGGTATCAAAGGACAGTINS80bpAGGTTAGAATGAAGGATGGGCAT TTGCTGAGCAAAATTAAGGGAACAAG**G**GACAGGTGGGAGTGTGGGGATCCAGGT TTCTGAGCTGAGATGAGCTGGGG**TGAGC**CAGGTAAGAGTGTGGGAACCCAGTC TTCCTGGTTGTTAAAGAATGGTATCAAA**T*****G***CAGGCAGAGTAGCTATAGGGCAGCCAG TTGAGAGCCCTAGTAAGCGAGGCTCTINS98bpGGCAGAGCAGCTATAGGGCAGCCA AACTCTACTGCCTACACTGGACTGTTCT**G**GGTGCCAGGACAGGTACAAGTTTAGTAG GTTTAATGAATTTGAAGTTGCCA***A***TAAA**T**ACAGGTAAGCAGGGACAGGTGGAAGTGT	GCTAAGCTAAACTAGGCTGGCTTAACCG:CCGGGTGAGCAAATACAAGGGAACTGAT TAGCTGAGATGGGGTGAGATGGGGTGAG:AGAGAAGCTGAGGCAGGTAAGAGTGTG CCACAGCTGTACAGAATTGAGAAA***T***AA**TA*T***AGGTAAG***T***AGGGACAGGTGGAAGTGT GCTAAACTAGGCTGGCTTAACCG:CCGGGTGAGCAAATACAAGGGAACTGATG TGGAAGAAAAGATGTTTTTAGTTTTINS215bpCCAGGCAGAG**C**AGCTATAGGGCAG ACTCTCCAGCCACAGTAATGACCCA**GA**GCAAATACAAGGGAACTGATGGCAA AATTAAGGGAACAAGGTTGAGAGC**C**AGCCAGGACAGGTGGGAGTGTGGG TCAGCTATGCTACGCTGTGTTGGGGT**GA**ACTGATGGCAAATGGAAGGGCAGGGACC TGAGATGGGTGGGCTTCTCTGAGINS233bpCAGGGGCAGGTTAGAATGAAGGAT GGTATGGATACGCAGAAGGAAGGCCACA**G**GAAGAATGCAGATCCAAACAGAAG
Mouse #2	AATGACCCAGACAGAGAAAGCCAG**ACT**GATGGCAAATGGAAGGGCAGGGAG TAATGACCCAGACAGAGAAAGCCA:CAAGACAACTAGAAGTGTGTGAA AAAGCATGGCTGAGCTGAGATG**GG**GGAGCCAGAACAGGTGGGAGTGTG TGAGGTGATTACTCTGAGGTAAGCAA:TACATACGGGTAAGCAGGGACAGGTG GAATTGAGAAAGAATAGAGACCTG**C**CCAGACTAAATGGCTACAGAGAAGCT GAAGGCCAGACTCATAAAGCTTGCT**GA**CAACTAGAAGTGTGTGAATCCAGG GCAGAAGGAAGGCCACAGCTGTACA*T*AGGCAGGTAAGAGTGTGGGAACCC AACTCAATGTGGTTTAATGAATTTGAAINS87bpTAGAGGAACAGGGGCAGGT GCTCTAAAAAGCATGGCTGAGCT**GAG**CCAAGACAACTAGAAGTGT TACTGCCTACACTGGACTGTTC**TGAGC**AAATACAAGGGAACTGATGGCA	GGCCACAGCTGTACAGAATTGAGA**AAGAAT**GGGGATCCAGGTGCTGCAGCTACAGG AAAGGACAGTGCTTAGATCCGAGGTGA:CCAGGACAGGTGGGAGTGTGGGGATCC AGAATAGAGACCTGCAGTTGAGGCCAG**CAGGT**AAGCAGGGACAGGTGGAAGTGT GGGGCTGGGGTATGGATACGCAGAAGG**AAGG**GAACTGATGGCAAATGGAAGGG CTACTACATTCTTGATCTACAACTC**AATG**AAGGATGTGCATCCTGGGTGAGCAAAT AAAGCTTGCTGAGCAAAATTAAGGGAA:A**C**GGGCAGGTTAGAATGAAGGATGT ACTGAGGTGATTACTCTGAGGT**AAGCA**GAGGCAGGTAAGA**C**TGTGGGAACCC AGAAAGCCAGACTCATAAAGCTT:TGCCAGGACAGGTACAAGTTTAGTAGTTA TAAACTAGGCTGGCTTAACCGAG**ATGA**AGGATGGGCATCCCGGGTGAGCAAATA TACAACTCAATGTGGTTTAATGAATTTGAA:CAGGTAAGGCAGGACTGGGGAGTCAA
Mouse #3	GCTTAGATCCAAGGTGAGTGTGAGAINS140bpTGGGGATCCAGGCAGTGTAGTTATA CTGAGATGAGCTGGGGTGAGCTCAGINS49bpTACAGGGAAGCTGAGGCAGGTA AGATCCAAGGTGAGTGTGAGAGGACAG:TGGGGAGCCAGGACAGGTGGAAGTG GATACGCAGAAGGAAGGCCAC**AGC**AGGGACAGGTGGAAGTGTGGAGACC TGTGAGAGGACAGGGGCTGGGGTATG**GA**GGAGCCAAGACAACTAGAAGTGTGT TTCTCTGAGCGCTTCTAAAATGCGCINS31bpTACAGGGAAGCTGAGGCAGGTAAG AGGCTCTAAAAAGCATGGCTGAGCTG:TTAGGAGCAAGGACAGGGAAGCT AGAGCCCTAGTAAGCGAGGCTCTAAINS38bpTACAGGGAAGCTGAGGCAGGTAAGAG CAGAGAAGGCCAGACTCATAAAINS82bpTGCTGCAGCTACAGGTAAGCAGGGACAG GCTTAGATCCAAGGTGAGTGTGAGAINS140bpTGGGGATCCAGGCAGTGTAGTTATA	GGTATGGATACGCAGAAGGAAGGCCACAC**C**AGGTGGGACTGTGGGGATCCAGGT TAAAATGCGCTAAACTGAGGTGATT**A**AACCACAGAAGAGCAGGAGCTAA GGTATGGATACGCAGAAGGAAGGCCACAC**C**AGGTGGGACTGTGGGGATCCAGGT TGGATACGCAGAAGGAAGGCCACAG:AGGGTGCCAGGACAGGTACAAGTTT TAAAAAGCACAGCTGAGCTGAGATGG**G**GGAGTGTGGGGATCCAGGTAAGGCAGG TAGACTGAGCTGAGCTAGGGTGAGC**TGAG**GGATGGGCATCCCGGGTGAGCAAATACA GATGTTTTTAGTTTTTATAG**A**GGACAGGGAAGCTATAGGGAAACCA CTGAGCAAAATTAAGGGAACAAGGTT**GA**TGGGCATCCCGGGTGAGCAAATACAA GAGAAAGCCAGACTCATAAAGCTTGCTINS191bpGGACAGGTGGAAGTGTGGAGA
Summary		
Blunt	17%	28%
Nt. additions / insertions	33%	17%
1/2 bp microhomology	30%	31%
> 2 bp microhomology	20%	24%

Blunt junctions are indicated with "**:**", micro-homology in **bold**, mutations in *italics*, and nucleotide additions are underlined. Micro-homology at the junction was determined by identifying the longest region at the switch junction of perfect uninterrupted donor/acceptor identity. INS: insertion. Results from 3 mice per genotype are shown.

Table S5. List of oligonucleotides used in this study, Related to STAR Methods.

Genotyping

Primer name	**Sequence (5'→3')**	**Reference**
Prkcbp1_35576_5	GACCACAGCTCTTGCACAGG	*EMMA/ Wellcome Trust Sanger Institute*
ZMYND8_R2 (Rev)	AAGAAAACCCTGAGACCACC	*This paper*
MDV_p240 (Fw)	GTGCAAACGTGTTCAGTGG	*This paper*

CRISPR-Cas9 gene targeting

gRNA	**Sequence (5'→3')**	**Reference**
gZmynd8-1	AGAAAACGGCCCCGAAACGG	*This paper*
gZmynd8-2	AAGTCATTCCGTCCGTCCTG	*This paper*
gZmynd8 Nickase pair 1	GTCTTGGGGCGAATGGCCAT ATTAAAAAGAAAAAGAAACC	*This paper*
gZmynd8 Nickase pair 2	GACACTTAGCGTGATAAACC GAGACTGACATCGGAGCCAG	*This paper*
gAID	TGAGACCTACCTCTGCTACG	*This paper*
Ctrl gRandom	GCGAGGTATTCGGCTCCGCG	*This paper*
Ctrl gRandom	ATGTTGCAGTTCGGCTCGAT	*This paper*
g*53BP1* Nickase pair	CAGATGTTTATTATGTGGAT GAGTGTACGGACTTCTCGAA	*This paper*
g*Rif1* Nickase pair	AAGTCTCCAGAAGCGGCTCC GAAGACCCCTCGGTGCCTCC	*This paper*

Quantitative pCR

Aicda	**Sequence (5'→3')**	**Reference**
AID-F (Fw)	GAAAGTCACGCTGGAGACCG	*Xu et al., 2015*
AID-R (Rev)	TCTCATGCCGTCCCTTGG	*Xu et al., 2015*
pre-spliced GLT γ1		
MDV_g1-3b (Fw)	CAGGATCAATCCCAGCATTGGG	*This paper*
MDV_g1-1 (Rev)	CTGTGCTTGGATCACCACACTTCC	*Oruc et al., 2007*
pre-spliced GLT γ3		
MDV_g3-3 (Fw)	GTGGAACTCTAAGGTTTAGGAGTCAA	*Oruc et al., 2007*
MDV_g3-1 (Rev)	CTGTGGCTGCTCAACTTGGTACCTT	*This paper*
pre-spliced GLT γ2b		
MDV_g2b-3 (Fw)	GTTGACCTGACCTAGAGACTGGTGGAC	*Oruc et al., 2007*
MDV_g2b-1 (Rev)	CTTTCTTTCAGCTTCATTCATGGAAC	*Oruc et al., 2007*
post-spliced GLT γ1		
Ig1 (Fw)	GGCCCTTCCAGATCTTTGAG	*Muramatsu et al., 2000*
Cg1R (Rev)	GGATCCAGAGTTCCAGGTCACT	*Muramatsu et al., 2000*
post-spliced GLT γ3		
Ig3F (Fw)	TGGGCAAGTGGATCTGAACA	*Muramatsu et al., 2000*
Cg3R (Rev)	CTCAGGGAAGTAGCCTTTGACA	*Muramatsu et al., 2000*
post-spliced GLT γ2b		

MDV_p243 (Fw)	CACTGGGCCTTTCCAGAACTA	*Muramatsu et al., 2000*
MDV_p244 (Rev)	CACTGAGCTGCTCATAGTGTAGAGTC	*Muramatsu et al., 2000*
post-spliced GLT μ		
ImF (Fw)	CTCTGGCCCTGCTTATTGTTG	*Muramatsu et al., 2000*
CmR (Rev)	GAAGACATTTGGGAAGGACTGACT	*Muramatsu et al., 2000*
3'RR hs1,2		
MDV_p324 (Fw)	CATTGAGCTCCGGCTCTAAC	*This paper*
MDV_p325 (Rev)	CAAGAGGACATGACAGGAGATG	*This paper*
3'RR 5' hs3b		
MDV_p314 (Fw)	CATTGAGCTCCGGCTCTAAC	*This paper*
MDV_p315 (Rev)	CCCCTGTAGGGATCCTCCTAAT	*This paper*
3'RR 3' hs3b		
MDV_p316 (Fw)	CATCCAGAGTCAAGGGGTGTC	*This paper*
MDV_p317 (Rev)	CTAGAACCACATGCTATCTAAGGGA	*This paper*

End resection assay

gRNAs	**Sequence (5'→3')**	**Reference**
gDSB-1	AGTTGTCATTGCTGAATATC	*This paper*
gDSB-2	CATGGATTTCTCCGGTGAAT	*This paper*
First round of PCR		
MA_p45 (Fw)	CTGTTAGAGCATGCTTAAGGG	*This paper*
MA_p42 (Rev)	TCACCATTAGGGCAAATGGC	*This paper*
Second round of PCR		
MA_p51 (Fw)	GTAGTTACTTGGCAGGCTCC	*This paper*
MA_p48 (Rev)	AAAGTCATTCCACAGTTTGAC	*This paper*

MutPE-Seq

First round of PCR	**Sequence (5'→3')**	**Reference**
QW_506 (Fw)	TCTACACTCTTTCCCTACACGACGCTCTTCCGATCTTCTCTGAGTGCTTCTAAAATGCG	*Wang et al., 2017*
QW_507 (Rev)	GTGACTGGAGTTCAGACGTGTGCTCTTCCGATCTTCACCCCAACACAGCGTAGC	*Wang et al., 2017*
Second round of PCR		
QW_501 (Fw)	AATGATACGGCGACCACCGAGATCTACACTCTTTCCCTACACGAC	*Wang et al., 2017*
QW_OutIndex (Rev)	CAAGCAGAAGACGGCATACGAGAT*6ntIndex*GTGACTGGAGTTCAGACGTGTG	*Wang et al., 2017*

GRO-Seq

Primer name	**Sequence (5'→3')**	**Reference**
RT-primer	/5Phos/GATCGTCGGACTGTAGAACTCTGAAC/idSp/CAAGCAGAAGACGGCATACGATTTTTTTTTTTTTTTTTTTTVN	*Ingolia et al., 2009*
oNTI201 (Fw)	AATGATACGGCGACCACCGACAGGTTCAGAGTTCTACAGTCCGACG	*Ingolia et al., 2009*
oNTI200 (Rev)	CAAGCAGAAGACGGCATA	*Ingolia et al., 2009*

Switch junctional analysis

First round of PCR	**Sequence (5'→3')**	**Reference**
5m3 (Fw)	AATGGATACCTCAGTGGTTTTTAATGGTGGGTTTAATATAG	*Di Virgilio et al., 2013*
gamma1R (Rev)	TGCCAATTAGCTCCTGCTCTTCTGTGG	*Di Virgilio et al., 2013*
Second round of PCR		
5m3-1 (Fw)	GGCTAAGAAGGCAATCCTGGGATTCTGG	*Di Virgilio et al., 2013*
gamma1R-1 (Rev)	CTCTTACCTGCCTAGCTTCTCTGTAGCC	*Di Virgilio et al., 2013*

SHM analysis

J_H4	**Sequence (5'→3')**	**Reference**
VHA (Fw)	ARGCCTGGGRCTTCAGTGAAG	*Sander et al., 2015*
VHE (Fw)	GTGGAGTCTGGGGGAGGCTTA	*Sander et al., 2015*
JH4_intron (Rev)	CTCCACCAGACCTCTCTAGACAGC	*Sander et al., 2015*
J_K5		
VK (Fw)	GGCTGCAGSTTCAGTGGCAGTGGRTCWGGRAC	*Rouaud et al., 2013*
JK5_PR (Rev)	AGCGAATTCAACTTAGGAGACAAAAGAGAGAAC	*Rouaud et al., 2013*